The use of CBERS (China-Brazil Earth Resources Satellite) to trace the dynamics of total suspended matter at an urbanized coastal area

Maria Fernanda Colo Giannini[1,2], Joseph Harari[3], Aurea Maria Ciotti[1]*

[1] Centro de Biologia Marinha - USP (CEBIMar/USP)
(Rod. Dr. Manoel Hipólito do Rêgo, S/N - Praia do Cabelo Gordo, São Sebastião - SP, 11600-000)
[2] Universidade Estadual Paulista - Campus do Litoral Paulista (Unesp-CLP)
(Praça Infante Dom Henrique, s/n - Parque Bitaru, São Vicente - SP, 11330-900)
[3] Instituto Oceanográfico da Universidade de São Paulo (IO-USP)
(Praça do Oceanográfico, 191, Butantã - São Paulo - 05508-120)

*Corresponding author: fe.cgiannini@gmail.com

Abstract

The distribution of organic and inorganic particles in the water column, or the total suspended matter (TSM), responds to local and remote oceanographic and meteorological processes, potentially impacting biogeochemical cycles. In shallow coastal areas, where particles have distinct origins and compositions and vary in different time scales, the use of remote sensing tools for monitoring and tracing this material is highly encouraged due to the high temporal and spatial data resolution. The objective of this work was to understand the variability of *in situ* TSM at Santos Bay (Southeastern Brazil) and its response to oceanographic and meteorological conditions. We also aimed to verify the applicability of the satellite data from CBERS-2 sensor in order to map the dynamics of TSM in this region. Our results have shown that the distribution of TSM in Santos Bay varied consistently with winds, currents and tidal cycles, with significant relationships emphasizing the role of south-western winds and spring tides. Neap tides and eastern winds, along with rainfall, play an important role in the input of organic matter into the bay. In conclusion, our analyses showed that the main patterns observed *in situ* regarding the responses of TSM to the ocean-meteorological processes could be reproduced in the CBERS-2 satellite data, after simple and standard methods of images processing. TSM data retrieval from CBERS-2 or other satellite sensors were shown to be feasible, becoming an essential tool for synoptic observations of the composition and quality of water, especially at urbanized and impacted coastal areas.

Descriptors: CBERS program, Santos Bay, Remote sensing, Suspended matter.

Resumo

A distribuição de partículas orgânicas e inorgânicas na coluna d'água, ou o material em suspensão total (MST), responde a processos oceanográficos e meteorológicos locais e remotos, que potencialmente impactam processos biogeoquímicos. Em áreas costeiras, onde partículas possuem diferentes origens e composições e variam em diferentes escalas de tempo, o uso de ferramentas de sensoriamento remoto para monitoramento e mapeamento desse material é altamente indicado devido à alta resolução temporal e espacial dos dados. O objetivo desse trabalho foi compreender a variabilidade do MST *in situ* na Baía de Santos (sudeste brasileiro) e sua resposta a condições oceanográficas e meteorológicas. Buscou-se também verificar a aplicabilidade dos dados de satélite do sensor CBERS-2 a fim de mapear a dinâmica do MST na região. Nossos resultados mostraram que a distribuição do MST na Baía de Santos variou consistentemente com os ventos, correntes e ciclos de maré, com correlações significantes que enfatizam o papel de ventos de sudoeste e da maré de sizígia. Marés de quadratura e ventos de leste, somados à precipitação, possuem papel importante na entrada de matéria orgânica na baía. Como conclusão, nossas análises mostraram que os principais padrões observados *in situ* em relação às respostas do MST aos processos meteorológicos e oceanográficos poderiam ser reproduzidas nos dados do satélite CBERS-2, após métodos padrões de processamento de imagens. A obtenção de dados de MST a partir do CBERS-2 ou outros sensores satelitais mostrou-se viável, tornando-se uma ferramenta essencial para observações sinóticas da composição e qualidade da água, especialmente em áreas costeiras urbanizadas e impactadas.

Descritores: Programa CBERS, Baía de Santos, Sensoriamento remoto, Material em suspensão.

Submitted on: 26/08/2016

Approved on: 22/01/2017

http://dx.doi.org/10.1590/S1679-87592017135006502

INTRODUCTION

Understanding the sources, sinks and transport of materials in aquatic environments is important, especially in regions that have been substantially altered by human occupation. In coastal and estuarine regions, water quality may be inferred from optical properties such as turbidity and surface reflectance (BUKATA et al., 1995), both of which are affected by the concentration and quality of particulate and dissolved materials and their respective spectral interaction with the solar irradiance (see IOCCG, 2000). The color of water can be measured either *in situ* or through remote sensing techniques and this information can be used for water quality studies and management once appropriate models are applied (GREEN et al., 2000; PHINN et al. 2005). In coastal waters, the total particulate suspended matter has fundamental importance in light scattering and reflectance (DEKKER et al., 2001), and consequently water transparency and its consequence for local primary productivity rates. Nonetheless, specifically in the green and blue portions within the visible bands, the colored dissolved organic matter, known as CDOM, tends to dominate water optical properties via light absorption (e.g. BOWERS et al., 2004). It is expected, therefore, that remote sensing techniques can provide information regarding the relative proportion of particulate and dissolved constituents affecting the optical signal of water bodies.

Santos Bay (Figure 1; 24.01°S and 46.35°W) is located on the southern coast of São Paulo state (SE Brazil) and comprises an urbanized estuarine complex where extensive tourism, industrial and fishing activities take place. It occupies an area of 30 km², with average depth of 15 m, and faces S-SE (DHN, 2003). The largest Brazilian commercial port and a number of plants are situated adjacent to the main estuarine channel. Because of that, Santos Bay receives organic and inorganic materials from several sources, which include estuarine outflows, sewage runoff (e.g. BUCCI et al., 2012) and a submarine sewage outflow (ABESSA et al., 2005), as well as adjacent coastal and continental shelf waters.

Meteorological conditions are expected to affect the TSM (total suspended matter) dynamics in Santos Bay and adjacent waters. At this region, mesoscale atmospheric circulation is modulated by the South Atlantic Subtropical High Pressure Center and its interaction with the Sub Polar Low Pressures (HARARI et al., 2008). Typically, moderate Easterly winds predominate year-round in the study area, but the passage of cold fronts leads to stronger Southern winds. The intensity and duration of these instabilities vary throughout the year, but they tend to be more frequent and stronger during winter (HARARI et al., 2006). A study during the period of 2 years have shown that the normal monthly mean sea levels have a maximum in April - May and a secondary maximum in August - September, which are related to steric effects in summer (volume increase) and cold fronts in winter, respectively (HARARI et al., 2008). During summer, precipitation rates tend to be higher at the coast of São Paulo (CPTEC/INPE, 1999; 2000), affecting TSM dynamics in this region (MOSER et al., 2005), as TSM is partially driven by discharge from two main estuarine channels, the São Vicente and Santos channels, to Santos Bay (see Figure 1). At timescales of hours and days, resuspension of bottom sediments may also become important during strong current tides or wind-driven currents (e.g., ALFREDINI et al., 2008). Nonetheless, the influence of local and remote meteorological events on the distribution and resuspension of TSM remains unknown at Santos Bay.

The complexity of processes regulating TSM supply and transport in estuarine environments reinforces the necessity of broad-range monitoring and management programs. Ideally, *in situ* samples taken at short timescales should be coupled with circulation data and numerical models of TSM transport encompassing the main local drivers. However, high temporal and spatial scale data sampling at dynamic and urbanized areas is problematic and accordingly, remotely sensed data from satellites is becoming more widely adopted (DEKKER et al., 2001; SHI; WANG, 2009; MILLER et al., 2011; ONDRUSEK et al., 2012). A series of sensors has been used to retrieve TSM in aquatic environments, such as the TM (Thematic Mapper) sensor, on board the LANDSAT (30 m resolution and 16 days overpass), the Moderate Resolution Imaging Spectroradiometer (MODIS) sensors from AQUA and TERRA satellites (1km resolution and daily overpass) and more recently, the SENTINEL Program was launched by ESA (European Space Agency), in order to continue the ongoing Earth observation missions (https://sentinel.esa.int/). The CBERS (China-Brazil Earth Resources Satellite) program series, used in the present study, was launched in 1999 by the Brazilian National Institute for Space Research (INPE) (http://www.cbers.inpe.br/). These satellites carry sensors with spectral and spatial resolution similar to those of the Landsat/TM sensors.

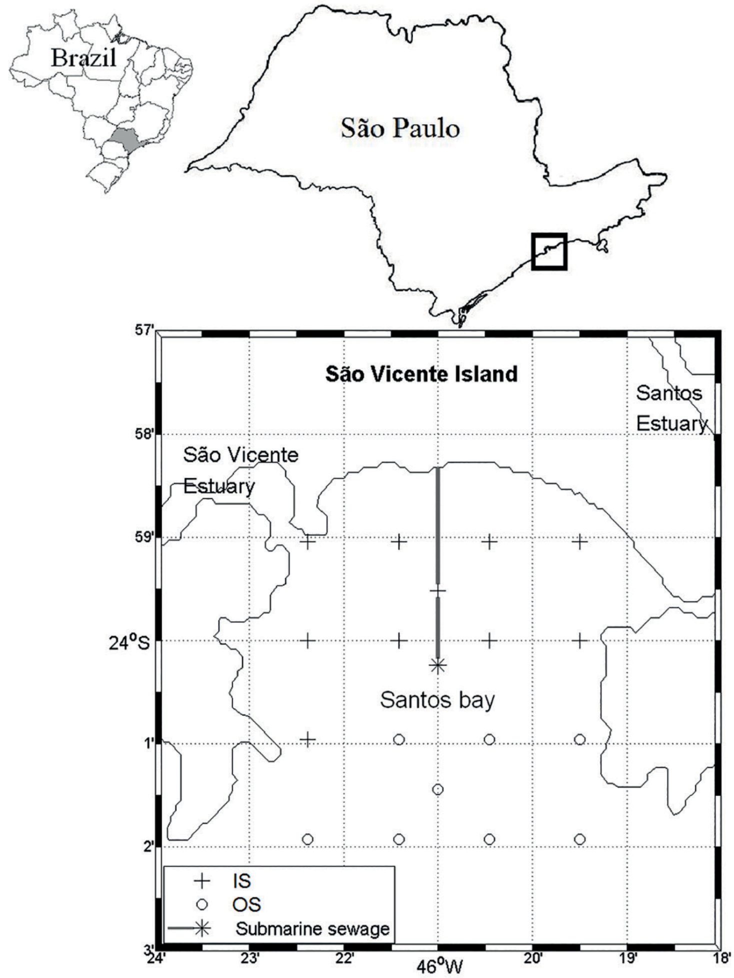

Figure 1. Santos Bay (São Paulo State, Brazil) and the oceanographic stations occupied during the study. The IS (inner portion, crosses) and OS (outer portion, circles) stations were separated according to the 10m isobaths. The oceanographic stations were repeated in all sampling campaigns (details in the text).

CBERS's CCD (Charge Coupled Device) sensors have five spectral bands, with spatial resolution of 20 m and overpasses every 26 days.

Due to the importance of remote sensing techniques for the management of coastal waters, the goal of the present work was to characterize patterns of TSM distribution in Santos Bay in relation to tides, precipitation and wind-driven currents. We also investigated the feasibility of remotely sensed estimates of TSM from the CBERS satellite to reproduce patterns observed *in situ.* Rather than a ground truth validation, due to the lack of simultaneous *in situ* and satellite data, our approach was to compute a TSM index for each available image, based on published algorithms, in order to detect robust spatial patterns of TSM.

MATERIAL AND METHODS

In situ data

Water samples were collected at 20 points distributed uniformly throughout Santos Bay (Figure 1). The sites were visited during eight scientific cruises carried out in March and August 2006 and March and September 2007. Each cruise was completed in about 8 hours, using two small vessels simultaneously: one dedicated to sample stations at the inner sector (IS stations) and the other at the outer sector of the bay (OS stations). In each of the above-mentioned months, two sampling campaigns were carried out: one at spring tide and other at neap tide (Table 1). Water samples were collected at the surface and at 1-2 meters above the bottom. Salinity was estimated in

Table 1. *In situ* data of TSM (Total suspended matter), OM (Organic Matter), Salinity, Wind velocity and direction (four days average, including sample day) and precipitation (six days average) in Santos Bay.

Date and Tide	Depth	TSM (mg/L) (mean±std)	OM(%) (mean±std)	Salinity (PSU)	Wind (m/s) and direction	Precipitation (mm/day)
2006 March 07	Surface (n=18)	36.3±10.3	29.5±4.1	31.92	1.6 – NW	5.38
(neap)	Bottom (n=17)	35.2±9.7	25.1±4.4	33.91		
2006 March 15	Surface (n=20)	57.1±17.9	25.7±3.8	33.15	2.25 – SE	4.42
(spring)	Bottom (n=19)	67.5±27.7	22.9±3.5	34.70		
2006 August 16	Surface (n=19)	65.9±5.1	28.0±1.6	32.84	1.9 – N-NE	0.00
(neap)	Bottom (n=15)	69.4±8.8	26.5±2.2	34.17		
2006 August 25	Surface (n=19)	69.2±14.0	25.7±2.7	32.65	2.41 – E-NE	1.57
(spring)	Bottom (n=18)	88.6±38.8	22.9±1.8	34.14		
2007 March 13	Surface (n=20)	37.7±8.4	33.5±7.8	31.55	1.32 – N-NE	5.54
(neap)	Bottom (n=20)	37.3±10.8	26.7±6.0	34.43		
2007 March 20	Surface (n=19)	27.2±10.0	30.3±7.3	32.17	1.6 – NW	21.34
(spring)	Bottom (n=19)	33.0±12.6	27.3±4.3	33.98		
2007 Sept 04	Surface (n=17)	12.3±8.4	41.3±14.6	27.87	2.92 – E-SE	0.00
(neap)	Bottom (n=18)	15.9±8.7	28.4±6.0	28.99		
2007 Sept 11	Surface (n=19)	13.3±16.1	34.6±12.7	28.37	2.87 – SE-NE	0.00
(spring)	Bottom (n=13)	16.6±12.3	24.1±8.0	30.73		

laboratory using an Autosal salinometer (BECKMAN model RS10) and CTD casts were performed at the OS stations.

A total of 290 samples were analyzed by gravimetric methods to measure TSM concentration (APHA 1985). Between 100 and 500 ml of water were filtered through numbered GF/F filters, previously dried at 60°C overnight and weighted. Filtrations were performed immediately after sampling, using a vacuum system and low pressure. In the laboratory, samples were dried at 60°C for 24 h, and then weighed using an analytical scale (0.001g precision); this procedure was repeated at least three times. The organic contents of each filter were combusted during 6 hours, at 500°C, and the filters were re-weighed at least three times. Among repeated weightings, the filters were stored in tightly closed containers with silica gel pellets, and reported values are means. TSM was computed as the difference between the weight of dried material and the initial weight for the unused filter, while the percentage of organic matter (%OM) was computed from the ratio between the combusted and the dried weight. Several clean filters were also processed to detect possible contamination.

Relationships between TSM and %OM variations and environmental and meteorological conditions were derived for sixteen groups of both surface and near-bottom data (i.e., 8 sampling dates and two sampling depths). A three-way ANOVA was performed to verify the differences of TSM and %OM distribution between the factors: sampling date, tidal condition during sampling date (neap and spring) and sampling depth (surface and near bottom). The homogeneity of variances was tested with the Bartlett method and Tukey's test was used a posteriori to verify the significance of the differences and interactions found between factors, with a confidence limit of 95%.

Meteorological data and modeled currents

Meteorological data were obtained from the global atmospheric model developed by the National Center for Environmental Prediction/National Center for Atmospheric Research (NCEP/NCAR) (KALNAY et al., 1996). The data were used to represent atmospheric conditions in the study area in mesoscale (see HARARI et al., 2008 for details). Model outputs from 2005 to 2008 at the closest grid point of NCEP/NCAR model to the Santos estuary (25°S 47.5°W) include 6-hour resolution wind velocity and direction, air temperature, atmospheric pressure and precipitation rates. In order to statistically relate our results to the mesoscale data, mean *in situ* values were computed for the entire bay. In addition to the model outputs, we also obtained local precipitation rates (mm/day) data from a rain gauge station located near the Santos estuarine channel (23°55'41.2"S and 46°18'09.6"W). This rain gauge station provides daily average rainfall data, and to relate the rainfall with *in situ* variables, data from 5 days were averaged (4 days preceding the campaigns plus the sampling day).

Current speed and direction were estimated by the hydrodynamic numerical model developed by HARARI et al. (2006), using the meteorological data from NCEP/NCAR as input, and also the mean sea level oscillations derived from observations at a local tidal station (Torre Grande; 23°56.95'S 46°18.50'W). Local tidal records (2005 and 2006) were used to compute mean sea levels using a low-pass filter based on running means (GODIN, 1972). Sea level harmonic decomposition (FRANCO, 1988) yielded components M2 and S2 with ranges of 0.37 m and 0.24 m, respectively. The hydrodynamic model computed hourly currents speed and direction (E-W and N-S components) for 2006 and 2007, for a grid inside Santos Bay. Modeled currents and measured TSM were compared with the smallest time lag for each station.

Satellite image acquisition, processing and quality control

A total of 14 images from the CBERS-2 CCD sensor, containing the entire Santos estuarine complex and the adjacent inner continental shelf, were acquired at http://www.dgi.inpe.br/CDSR/. The initial quality control consisted of inspections for cloud coverage, geographical displacement offset or acquisition failures among different spectral bands, which eliminated seven images. Geographical and atmospheric corrections, using the Simulation of the Satellite Signal at Solar Spectrum atmospheric correction code (5S, see TANRÉ et al., 1990), via SCORADIS were performed to convert digital numbers to physical units of Bidirectional Reflectance Factors (BRF). These corrections eliminated 5 additional images, thus only the remaining 2 images could be fully processed (see steps at Figure 2). All steps were performed with Spring 4.3.3 software and packages, freely available at http://www.dpi.inpe.br/spring.

Spatial variability of surface TSM from remote sensing data

Initially, we estimated surface TSM concentration through the model proposed by DEKKER et al. (2001). This algorithm (Equation 1) was developed for a coastal environment with similar characteristics to the study area, regarding TSM concentrations and sources, and is an exponential function of the average between bands 2 and 3 (x, red BRFs) of the TM-sensor (Landsat satellite), following:

$$TSM = 0.7581\ e^{61.683x} \quad (1)$$

Although Equation 1 provided realistic results (see below), we chose to study the spatial heterogeneity of TSM at Santos Bay on maps of the natural logarithm value of the average between bands 2 (0.52-0.59µm) and 3 (0.63-0.69µm) from CBERS (hereafter denominated TSM index) in order to keep the fundamentals proposed by DEKKER et al. (2001), without relying on their regional coefficients. TSM indexes were computed with LEGAL, a program language available at the Spring software, and the resulting images were then segmented and classified using a non-supervised classification, obtained through the algorithm called as Isoseg, that uses the Mahalanobis distance to identify regions of similarity (SANTOS et al., 2010). Segmentation yielded regions with continuous pixels showing spectral uniformity. In other words, distinct regions of the estuarine complex and Santos Bay were thus classified according with their similar TSM index values, which varied with the surface reflectance in the bands 2 and 3 of the CBERS-2 CCD sensor. It is important to note that the classification step is used for spatial comparisons in a particular image and not among distinct images.

RESULTS

In situ data

Average values of total suspended matter (TSM) were higher near the bottom, while the percentage of organic matter (%OM) showed an inverse trend, probably due to the combination of inorganic matter resuspension and surface inputs of organic estuarine material (Table 1). Contrary to previous observations (MOSER et al., 2005; SCHMIEGELOW et al., 2008), we found no clear relationship between %OM and 5-day averages local precipitation.

Mean surface TSM concentration and %OM showed direct (r^2=0.75) and inverse (r^2=0.78) relationships respectively with salinity (Figure 3a), while no relationships were observed near the bottom. The ANOVA analysis suggested significant interactions between both TSM and %OM, with the sampling date, the tidal cycle and depth (Table 2), reinforcing the role played by local sediment resuspension as a TSM source during the winter, when near-bottom TSM values were statistically higher than those observed at the surface, regardless the sampling period. Both sampling date and depth were related to %OM, showing

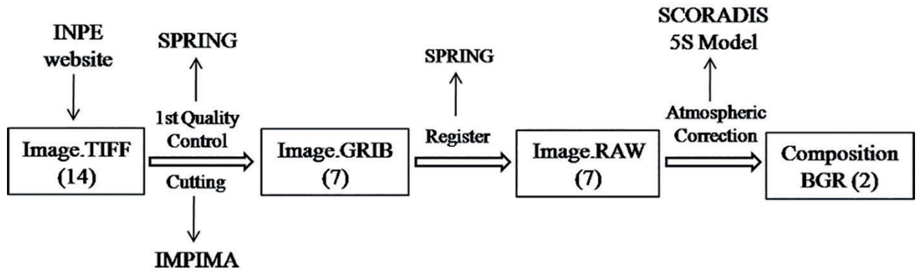

Figure 2. Diagram of the main procedures used during the quality control and images processing from CBERS satellite. The number of images analyzed in each processing steps are in brackets. The arrows indicate the software used in the processing stages.

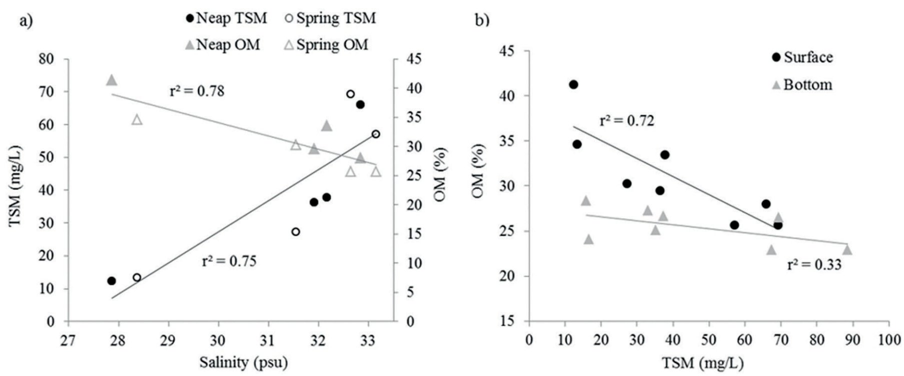

Figure 3. a. Linear regressions between the surface salinity and the percentage of organic matter (%OM) and total suspended matter concentration (TSM) (N=8). b. Linear regression between %OM and TSM for both depth layers.

Table 2. Three-way ANOVA for differences in TSM concentration and the %OM regarding three fixed factors: sampling date, tides and depth layer.

Effect	TSM		OM	
	F	p	F	*p*
Date	208.6	< 0.0001	14.52	< 0.0001
Tide	17.5	< 0.0001	16.42	< 0.0001
Depth	7.8	0.006	50.27	< 0.0001
Date*Tide	20.7	< 0.0001	1.15	0.329
Date*Depth	0.4	0.754	6.69	< 0.0001
Tide*Depth	3.8	0.053	1.12	0.291
Date*Tide*Depth	0.6	0.637	0.49	0.693

*values in bold indicate significance to α=0.95. F is the critical value of statistic and *p* is the error probability.

higher mean values at the surface than near-bottom, although only significantly in September 2007. An inverse relationship between the mean %OM and the TSM concentration at the surface was also observed (Figure 3b; $r^2 = 0.72$).

Salinity ranged from 27.8 to 34.7 (Table 1), with the lowest values observed during September 2007, suggesting a high continental runoff, although no precipitation was registered for the period. Differences between near-bottom and surface salinity values (hereafter called ΔSal) were likely driven by tides and the continental runoff. Higher ΔSal values were found at the shallow stations during the neap tide campaigns of March 2006 and 2007, following high rainfall events. During spring tides, ΔSal was lower due to intensification of local currents and vertical mixing.

Modeled meteorological and physical data

The atmospheric model computed monthly mean air temperature varying according to expected seasonal trends, from 17.4°C (± 3.8) in July to 22.6°C (± 1.9) in February (Figure 4). In March 2006, neap and spring tide cruises followed distinct degrees of atmospheric instabilities: previously to the spring tide campaign, atmospheric instability was observed on days 11 to 13 (Figure 4a), resulting in stronger and longstanding winds from the southern quadrant. In August 2006, both surveys also had contrasting atmospheric conditions, with rising air temperatures and Northern winds at neap tide sampling, while the spring tide campaign occurred after the passage of a cold front, with lower temperatures and intense Southern winds (Figure 4b). In March 2007, a number of weak frontal systems affected the study area (Figure 4c), generating low intensity Southern winds, while in September 2007, both sampling cruises occurred after stable conditions (Figure 4d).

The magnitudes of wind velocities were compared to the mean TSM concentrations. When data from September 2007 are excluded, mean TSM showed a clear and direct relationship with the wind speed data, which were averaged over the NCEP model outputs for four days preceding the sampling campaigns, plus the sampling day (Figure 5). Indeed, the dataset from both campaigns in September 2007 were unique: TSM concentrations, as well as the salinity values were noticeable low, while the %OM was high. Low salinity waters in the Santos Bay can occur during high estuarine discharges, but the relationships between salinity and the precipitation rates, both estimated by the NCEP model or observed at the local weather station, were negligible. The unexpected results from September 2007 do not seem to be related to the precipitation rates within the five-day interval considered in our analyses. Nonetheless, an intense estuarine contribution is unquestionable, that could be a result of persistent Eastern winds or a response from heavy rainfall rates registered in August, either locally or from surrounding areas (e.g. São Paulo city) that is drained to the estuarine complex.

Sea level and tidal records for 2005 and 2006 used as boundary conditions on the hydrodynamic model, showed mean sea levels varying from 0.49 m to 0.61 m. Model estimates of tidal currents, at the central point of Santos Bay, resulted in mean values of 0.07±0.04 m/s along the water column, with relatively small and typical estuarine residual currents: towards the open sea at surface and towards the continent close to the bottom.

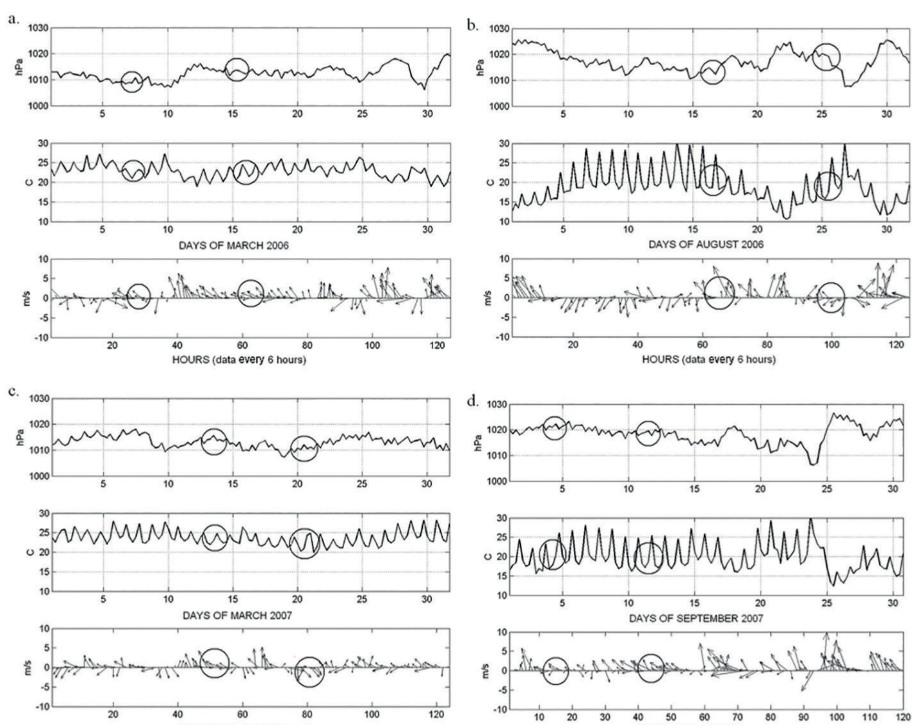

Figure 4. Results from the atmospheric NCEP/NCAR model for March 2006 (a), August 2006 (b), March 2007 (c) and September 2007 (d): Atmospheric pressure (hPa), air temperature (C) and winds field at the sea surface (m/s). Circles indicate the sampling periods.

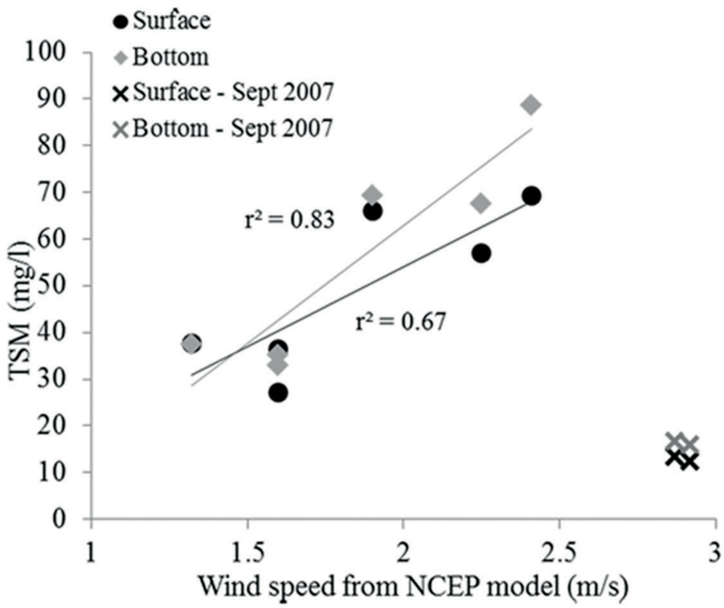

Figure 5. Linear regression between the modeled wind speed and the surface and near bottom averages of TSM concentrations (N=8). Data from September 2007 are neglected.

TSM concentration was related to the North-South components of the surface currents (Figure 6), with no significant relationship with the East-West component. Note that data from September 2007 were excluded from these regressions, and were performed separately for inner and outer sectors (IS and OS stations) to emphasize the role of bathymetry and the possible influence of sediment resuspension. Indeed, the shallower stations (IS) showed a stronger correlation between TSM and N-S wind velocities.

TSM satellite images

The processed images are from winter periods, 07/27/04 and 07/26/05 and the overpass time was around 10:00am. The 2004 and 2005 images are from neap and spring tides, respectively. Inside Santos Bay, mean red BRF (Bidirectional Reflectance Factors) varied between 3.3 and 5.7% (07/27/04 image), and between 4.1 and 6.3% (07/26/05 image), which yielded TSM concentrations from 5.91 to 36.3 mg/L, according to equation 1 (Figures 7a and 7c). The TSM *in situ* estimates had the same order of magnitude.

The non-supervised classification showed a high degree of heterogeneity for TSM indices within Santos Bay. In the 2004 image, three different classes were distinguished, while four groups were observed in the 2005 image (Figures 8b and 8d, respectively). True color composites are also presented to complement and aid the interpretation of the different classes obtained.

For the 2004 image, high TSM indexes were observed for shallow waters, probably driven by sediment resuspension, generating the first group (Table 4 and Figure 8b). The second group, including the northern edge of São Vicente estuary and the center of the bay, above the main submarine sewage outlet, showed intermediate TSM indexes. The third and larger group presented lower TSM index and included the main portion of the bay, adjacent coastal waters and the estuarine channels.

Distinct TSM distribution was observed in the 2005 image, where larger areas with high TSM indexes were observed extending to deeper portions of the bay, consistent with a more intense vertical mixing, that will be further discussed. A sharp contrast between the central portion of the bay and the adjacent coastal water with lower TSM indexes was also observed, suggesting the presence of a frontal zone. TSM indexes in this frontal region were similar to those found in the estuarine plumes. The last group was located in the São Vicente estuarine channel. This image was acquired during spring tide, with intense S-SW winds preceding the CBERS's overpass (Table 3).

The classification procedures for both images showed good agreement with tidal and meteorological conditions

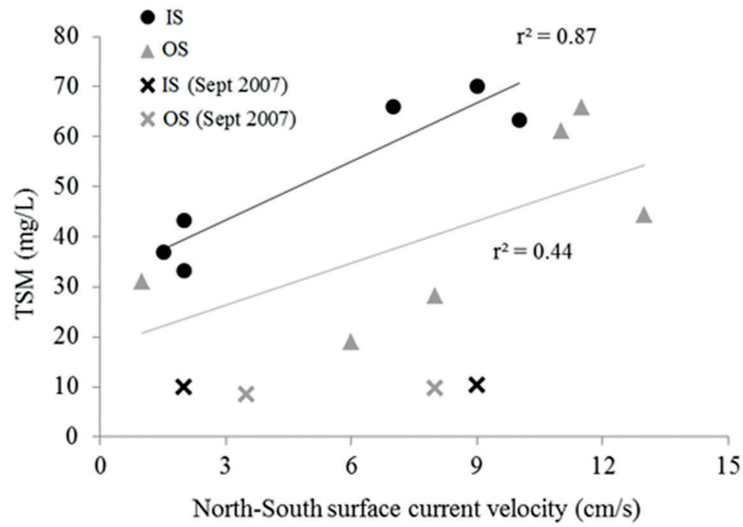

Figure 6. Linear regression between surface TSM averages and the North-South surface current velocity. September 2007 data are excluded of the linear trends, as in figure 05. IS and OS refer to Inner and Outer portion of the bay, respectively.

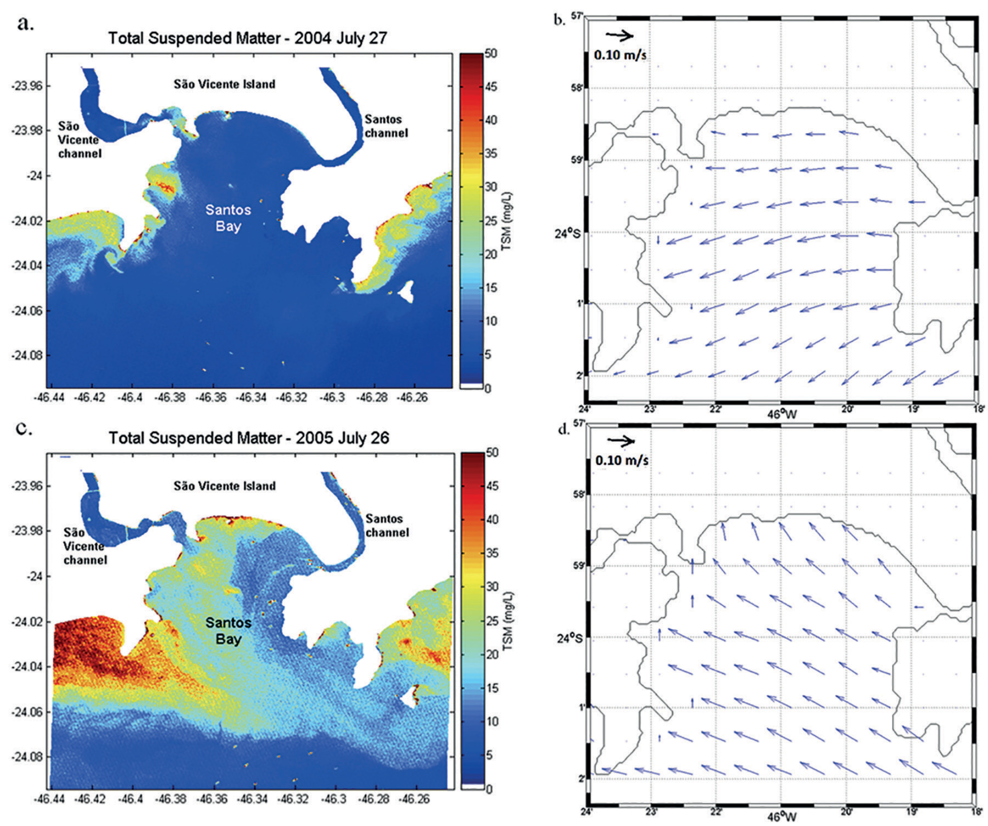

Figure 7. CBERS satellite images processed using the Dekker's algorithm to provide TSM concentration in mg/L (a, c) and the respective direction of the daily averaged surface currents modeled for the bay (b, d).

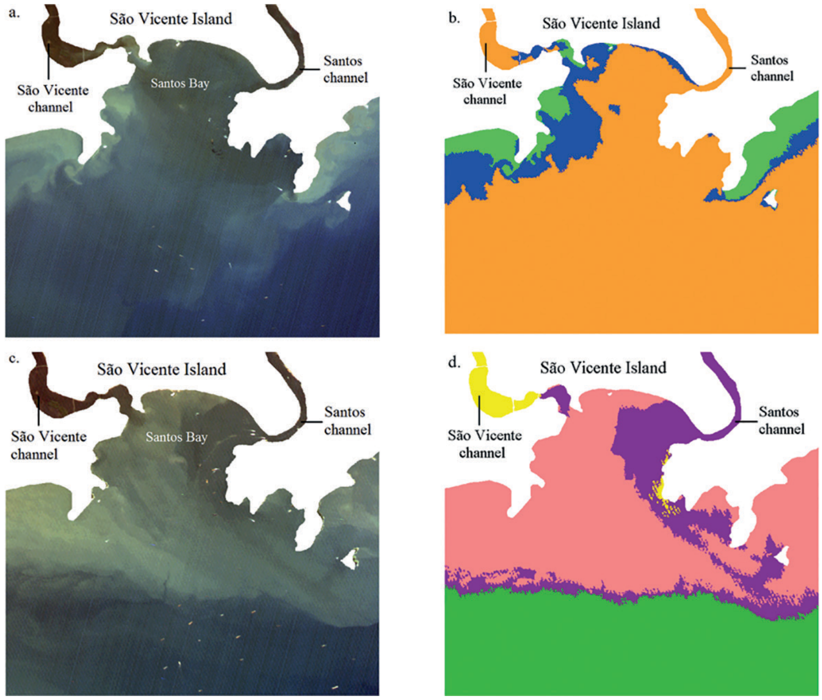

Figure 8. True color (BGR) composites for July 27 2004 (a) and July 26 2005 (c) CBERS satellite images. Non-supervised classification of the TSM index was applied for the same images (b, d). Colors are arbitrary and represent the groups from Table 4 (images must be individually analyzed, considering that the colors are not comparable). For July 27 2004: green, blue and orange – groups 1, 2 and 3, respectively. For July 26 2005: pink, green, purple and yellow – groups 4, 5, 6 and 7, respectively.

Table 3. Wind velocity and direction four days before the images acquisition.

Date	Velocity (m/s)	Direction
07/24/04	2.35	SE
07/25/04	2.44	SE
07/26/04	1.84	E
07/27/04 (overpass)	2.36	E
07/23/05	1.59	N-NE
07/24/05	2.14	N-NE
07/25/05	1.93	W-S
07/26/05 (overpass)	2.46	SE

(Table 4). Major current and wind components were in the E-W quadrant (Figure 7b and Table 3, respectively), favoring Santos estuary outflow and localized resuspension over the western margin of the bay. Although wind and current magnitudes were similar to those of the previous year, the 2005 image was acquired during spring tide, and both the NW-flowing current and wind from S-SE origin were the most significant (Figure 7d and Table 3, respectively), suggesting intense vertical mixing.

DISCUSSION

Dynamics of TSM in Santos Bay and its adjacent estuarine complex

Water quality management in coastal waters can benefit from synoptic descriptions of spatial distributions of suspended and dissolved matter. In aquatic environments with complex circulation and various sources of materials, remote sensing techniques become an essential tool for monitoring programs (e.g. FISCHER; DOERFFER, 1987; DOERFFER et al., 1989). Our results showed that the *in situ* distribution of total suspended matter (TSM) at Santos Bay varied consistently with winds, currents and tidal cycles. Additionally, our analyses showed that the main features and dynamic patterns observed *in situ* were reproduced in two CBERS satellite images, after the application of simple and standard processing procedures.

Santos Bay waters receive organic and inorganic compounds from several sources, including two main estuarine channels, a number of urban drainage channels, a submarine sewage outlet and the adjacent inner continental shelf. Wind and tidal-driven vertical mixing

Table 4. Classified groups and the environmental conditions close to the overpass.

Date	Precipitation	Wind	Tide	Classified groups
07/27/04	Low precipitation in the days before the overpass	Predominant direction: from E-SE. Moderate velocity in the days close the overpass	Neap (flood tide)	1. Sediment resuspension and bottom reflectance 2. Intermediate reflectance (São Vicente Bay and submarine sewage plume) 3. Santos Bay and adjacent coastal water
07/26/05	Relatively high precipitation a day before the overpass, however just around noon	Predominant direction: from N-NE until 07/25/05, switching to stronger winds from S-SE	Spring (ebb tide)	4. Santos Bay 5. Adjacent coastal water 6. Intermediate reflectance (front and estuarine plume) 7. São Vicente estuarine channel

resuspend bottom sediments (MOSER et al., 2005) and additionally, since 2002, the Santos estuarine channel has been continuously dredged to allow commercial ship access to the port of Santos, which also promotes resuspension. On some occasions, the influence of the submarine sewage outflow at the central portion of the bay was evident as higher TSM and %OM values.

The statistical analyses have shown that local tidal dynamics played a great role in the TSM and %OM distribution in Santos Bay. During spring tides, enhanced water column turbulence likely caused resuspension of bottom sediments rich in inorganic compounds, while during more stable conditions at neap tides, TSM concentration decreased and %OM increased. Hence, the very low TSM values registered in September 2007 could also result from a process that avoids bottom sediment resuspension reaching the surface, such as a likely decrease in wave height, or the presence of a strong, persistent and deep halocline.

Wind dynamics are a major factor affecting the physical structure and flushing characteristics of estuaries (GEYER, 1997). Wind direction and velocity influences both the extension of estuarine plumes and their constituent loads, including TSM (SIEGEL et al., 1999). Offshore winds can spread estuarine plumes (DURAND et al., 2002), and the combination of wind, river flow and tides will control plume dynamics. In Santos Bay, we found strong relationships between wind speed and TSM distribution, with rainfall apparently playing a secondary role. The effects of waves can be another important factor determining TSM concentration in shallow areas (PULS et al., 1994) and as Santos Bay is oriented southward (Figure 1), the importance of wave action during southern winds becomes important, however, no information about wave fields is available for the studied period. Especially during winter, the frequency and intensity of cold frontal systems significantly increases wave activity inside the bay (e.g. CASSIANO et al., 2012); thus, TSM concentration in Santos Bay can also be related to remote wind fields. Further *in situ* observations and modeling exercises focusing on the relative importance of waves to TSM transport are still necessary.

In general, *in situ* TSM concentrations were strongly related to the wind fields only when data from September 2007 were excluded. In these cases, salinity and TSM concentrations in Santos Bay waters were not only the lowest of all campaigns, but were also lower than previously published values. Both the mesoscale model estimates and the local *in situ* results of precipitation rates were low or absent and thus unable to explain the observed decrease in salinity. One possible explanation for this salinity anomaly is an increase in freshwater contributions from the Henry Borden hydroelectric power plant, located in the city of Cubatão, 14 km uphill from Santos. The power plant captures water from reservoirs in the area of São Paulo city, and deposits it in the Santos estuary (GASPARRO et al., 2008). Since a high precipitation event was registered in the city of São Paulo two days before the neap tide sampling (CPTEC/INPE 2007), outflows from the power plant to the estuary could explain the anomalous data. Unfortunately, no official discharge data from Henry Borden were available for this period; however, the importance of the Henry Border plant in the study area is discussed in BUCCI et al. (2012). Regardless the source of freshwater, our results showed a significant estuarine contribution in both September 2007 campaigns. Chlorophyll concentrations were low during these periods (MOSER et al., 2012), which also corroborate the increase in the flushing volume.

In general, both the *in situ* and the satellite image data emphasized the importance of wind speed on total suspended matter distribution in Santos Bay. Such patterns have been observed in other similar environments. FORGET and OUILLON (1998), for example, have shown how the TSM distribution patterns in the Mediterranean varied according to wind-driven currents. Also, the combination of satellite images and numerical models during a period of dredging in a port in Finland indicated that TSM patterns depend not only on the dredging itself, but also on wind-driven currents (SIPELGAS et al., 2006). In addition, TSM concentration in Santos Bay seems to vary with wind direction as well: winds from southern quadrant tend to increase overall turbulence and sediment resuspension to the water column, while winds form E-N quadrant tend to increase estuarine contributions and decrease TSM concentrations.

The use of CBERS satellite data to remotely assess the TSM dynamics

Data validation and spatiotemporal resolution are major obstacles for satellite-derived data in coastal waters. Often, the spatial resolution of remotely-sensed data is too low to describe important horizontal gradients of TSM in coastal areas and the temporal resolution is not high enough to follow short-time scale variability driven by tides, waves and atmospheric instabilities (NITTROUER; WRIGHT, 1994). AVHRR (Advanced Very High Resolution Radiometer), Landsat TM (Thematic Mapper), SeaWiFS (Sea-viewing Wide Field-of-view Sensor) and MODIS have all been used to map suspended sediment distribution in different environments. Both AVHRR and SeaWiFS have almost daily global coverage but their spatial resolution is low (1.1 km). Landsat has a 30m spatial resolution but low temporal scale (16 days cycle). MODIS sensors offer high acquisition frequency (almost daily) and better spatial resolution (250m to bands 1-2 and 500m to bands 3-7, respectively) and are therefore more suitable for monitoring smaller water bodies such as bays and estuaries (MILLER; MCKEE, 2004; MILLER et al., 2005). However, Santos Bay requires finer spatial scale data due to its reduced size. This data is available in Landsat and CBERS images and in a number of other sensors such as Quickbird, IKONOS and SPOT. In our work, CBERS data was used for convenience, and also to illustrate its potential to generate TSM products. Our results, however, are relevant for all sensors mentioned above.

The algorithm proposed by DEKKER et al. (2001), used to estimate TSM surface concentration from water leaving reflectance at red wavebands, is a semi-analytical formulation easily applicable for a number of available sensors. It is also based on well-known physical and optical theories. Simpler approaches are also possible, such as the one from MILLER and MCKEE (2004), also using red spectral bands (620-670 nm from MODIS/Aqua), which proposed empirical TSM algorithms for the Gulf of Mexico. The authors assumed that an increase in TSM concentration linearly increases water-leaving reflectance in the red band, an approach also used by SIPELGAS et al. (2006) for TSM determination in the Gulf of Finland. At Santos Bay, averaged TSM values estimated from DEKKER's algorithm were slightly lower than the *in situ* dataset presented here. This result is somewhat expected, once our maximum TSM concentrations were beyond the range used in their algorithm formulation (figure 7 in DEKKER et al., 2001). Nonetheless, estimated TSM values were within the same order of magnitude of our *in situ* data set, thus the development of regional algorithms using similar principles would be highly encouraged.

The classification process applied to the CBERS images showed a heterogeneity for our TSM indexes. The groups generated within a particular image were based on values of TSM indexes, with similar regions observed at Santos Bay, in the estuarine channels and the adjacent continental shelf waters. In the 2004 image, the waters inside the bay and the adjacent coastal waters were grouped into a unique class, suggesting low turbulence conditions and higher transparency (Figure 8b); these features were corroborated by the meteorological conditions in a scale of days preceding the overpass. On the other hand, the true-color composite (Figure 8a) suggests that the water with low TSM indexes found in the center of the bay were associated with a brownish water color forming a plume from the main estuarine channel towards the bay. This is probably a result of a very high contribution of Colored Dissolved Organic Matter (CDOM), which has been previously reported in this region (BUCCI et al., 2012; FERRARI et al., 2014), and could trace the estuarine discharge. In estuarine plumes, the decrease in TSM, or CDOM, towards offshore is not a simple process of dilution (OUBELKHEIR et al., 2006), particles size and their chemical composition will also change, leading to biogeochemical and optical changes (BUKATA, 2005; BURD; JACKSON, 2009; CHEN et al., 2005; FETTWEIS et al., 2006).

In the 2004 image only the very shallow regions presented high water-leaving reflectance on red bands (green patches at Fig 8b), suggesting mainly sediment resuspension, although contributions from bottom reflectance cannot be discarded (e.g., FORGET;

OUILLON, 1998). Two more features were observed in this image: first, the water inlet from Santos Bay through one side of the São Vicente estuarine channel, resulting from flood tide (blue patches), which generated a strong longitudinal TSM gradient across this small bay; the second feature is the clear localized plume over the underwater sewage outflow, where a diffuser launches the effluent to the surface. This plume was also detected in our *in situ* data, showing high TSM and %OM at surface for stations located near the outlet. Note that the sewage outlet is located near the bottom, where there is a diffuser, and it is expected that the discharge varies as a function of the rainfall. For these reasons, it is not expected that a visible surface plume will be always present.

The TSM classes formed in the 2005 image were distinct from 2004 image but were consistent with meteorological and tidal conditions during this satellite overpass. Waters in the center of the bay showed distinct TSM indices from those in the adjacent coastal waters, suggesting a more turbulent pattern in the bay (Figure 8d). The overpass on 07/26/05 occurred during spring tide, when higher turbulence and sediment resuspension are expected, as observed in the *in situ* dataset. Strong S-SE winds were recorded before the overpass (Table 3) and could increase turbulence. Due to the orientation of the Santos Bay mouth southwards, winds from the southern quadrant raise the sea level, piling water inside the bay, promoting increasing waves. Modeled surface currents (Figure 7d), predominantly to northwest, reinforced this hypothesis. As a result, a plume in the 2005 image can be clearly detected adjacent to Santos Bay by the strong TSM index gradient. Indeed, the detection of frontal zones has been a major achievement in studies using satellite images in estuaries (e.g., FORGET; OUILLON, 1998; MILLER; MCKEE, 2004).

The combination of ebb tide at the time of the overpass of the satellite and high precipitation rates the day before suggest that the class formed by intermediate TSM indices values in the 07/26/05 image probably originated from Santos estuarine channel discharge. It is interesting to note that waters from São Vicente and Santos estuaries show distinct colors in the RBG composite, suggesting distinct optical properties. The darker waters found in São Vicente estuary indicate higher amounts of CDOM. This constituent, usually estimated by its coefficients for light absorption, will have magnitudes inversely proportional to salinity, so that CDOM absorption coefficients are sometimes used as a tracer for freshwater input (e.g., FERRARI; DOWELL, 1998). CDOM is an optical component important in both the Santos and São Vicente estuarine channels (FERRARI et al., 2014). However, the true color composite (Figure 8c, d) suggests that their overall CDOM exports are optically distinct. The Santos channel receives a larger amount of industrial effluents (BRAGA et al., 2000) than the São Vicente channel, which receives larger proportion of domestic waste. The dynamics of both estuaries (flow, length and depth) are also different, which significantly impacts the origin and the distribution of TSM and CDOM in the entire estuarine complex.

FINAL CONSIDERATIONS

Our goal was to investigate the relationships between winds, tides and precipitation on TSM distribution and their organic matter content in Santos Bay. Statistical analyses have indicated that the surface TSM concentration seemed to be mainly driven by wind and tidal currents, probably due to resuspension of bottom sediments. The influence of tides and winds will be more significant during the passage of meteorological instabilities, when southerly winds promote higher turbulence inside the bay. Ultimately, estuarine discharges and waves can also influence the TSM dynamics due to the persistent E-W winds and currents, which can pile water inside the bay, increasing the estuarine outflows independently of the local rainfall rates. The patterns observed *in situ* regarding the dynamics of TSM controlled by oceanographic-meteorological conditions could be similarly reproduced through remote sensing analysis.

The use of CBERS satellite images processed with a semi-analytical algorithm for TSM concentration estimation provided results of the same order of magnitude of the *in situ* data. CBERS satellite data, once carefully processed and quality controlled, can therefore offer reliable products, such as the TSM dynamics for shallow coastal waters in high resolution. However, validating remote sensing products using ground truth methods is usually very challenging. Apart from cloud coverage issues, the combination of *in situ* samples and the spatial and temporal characteristics of the satellite data, desirable for a robust statistical treatment, is difficult to obtain. The acquisition of a significant number of replicates is equally problematic, unless moorings equipped with specific and calibrated sensors are operational for several years. The development of regional algorithms, both for particles and the dissolved organic matter, is highly encouraged as an important step for a better description of the optically active components in the water at this important urban coastal area. The analysis and interpretation shown in the present work can be extended to other satellite sensors, with higher spatial and temporal resolution, contributing to the studies in aquatic systems management and environmental monitoring programs.

ACKNOWLEDGEMENTS

The authors thank FAPESP by funding MFCG (project number 05/60602-8) and the entire CIRSAN project (Fapesp 03/13747-5) personal, especially Dr Sonia Gianesela and Dr Flávia Saldanha Correa from IO-USP. We particularly thank Dr. Flavio Ponzoni for the important contribution with some satellite images analysis. We thank Renato de Traglia Tonini and Fabiana Pestana Barbosa for their assistance during sampling campaigns and laboratorial analyses and we appreciate the detailed comments provide by Dr. J.V. Guerra in our manuscript. This research is a contribution of the NP-BioMar, CEBIMar, University of São Paulo.

REFERENCES

ABESSA, D. M. S.; CARR, R. S.; RACHID, B. R. F.; SOUSA, E. C. P. M.; HORTELANI, M. A.; SARKIS, J. E. Influence of a Brazilian sewage outfall on the toxicity and contamination of adjacent sediments. *Mar. Pollut. Bull.*, v. 50, n. 8, p. 875-885, 2005.

ALFREDINI, P.; ARASAKI, E.; AMARAL, R. F. Mean sea-level rise impacts on Santos Bay, Southeastern Brazil – physical modelling study. *Environ. Monit. Assess.*, 144, n. 1, 377-387, 2008.

APHA (AMERICAN PUBLIC HEALTH ASSOCIATION, inc.). *Standard Methods for the Examination of Water and Wastewater*. 16th ed. Washington: APHA, 1985.

BOWERS, D. G.; EVANS, D.; THOMAS, D. N.; ELLIS, K.; WILLIAMS, P. J. le B. Interpreting the color of an estuary. *Estuar. Coast. Shelf Sci.*, v. 59, n. 1, p. 13-20, 2004.

BRAGA, E. S.; BONETTI, C. V. D. H.; BURONE, L.; BONETTI FILHO, J. Eutrophication and Bacterial Pollution Caused by Industrial and Domestic Wastes at the Baixada Santista Estuarine System – Brazil. *Mar. Pollut. Bull.*, v. 40, n. 2, p. 165-173, 2000.

BUCCI, A. F.; CIOTTI, A. M.; POLLERY, R. C. G.; CARVALHO, R.; ALBUQUERQUE, H. C.; SIMÕES, L. T. S. Temporal variability of chlorophyll-a in the São Vicente estuary. *Braz. J. Oceanogr.*, v. 60, n. 4, p. 485-499, 2012.

BUKATA, R. P. J. H.; KONDRATYEV, K. Y.; POZDNYAKOV, D. V. *Optical Properties and Remote Sensing of Inland and Coastal Waters*. Boca Raton: CRC Press, 1995. 362 p.

BUKATA, R. P. *Satellite monitoring of inland and coastal water quality: retrospection, introspection, future directions*. Boca Raton: Taylor & Francis, 2005. 246 p.

BURD, A. B.; JACKSON, G. A. Particle Aggregation. *Ann. Rev. Mar. Sci.*, v. 1, p. 65-90, 2009.

CASSIANO, G. F.; RIBEIRO, R. B.; YASSUDA, E. A. Acquisition of wave data and modeling in Santos Bay, São Paulo, Brazil. In: *Proceedings of the 10th International Conference on Hydroscience & Engineering*. Orlando, 2012.

CHEN, M. S.; WARTEL, S.; TEMMERMAN, S. Seasonal variation of floc characteristics on tidal flats, the Scheldt estuary. *Hydrobiologia*, v. 540, p. 181-195, 2005.

CPTEC/INPE. Climanálise. *Boletim de Monitoramento e Análise Climática*, 1999, v. 14, n. 1-8. Available: <http://www.cptec.inpe.br/products/climanalise/capa1.html>.

CPTEC/INPE. Climanálise. *Boletim de Monitoramento e Análise Climática*. 2000, v. 15, n. 1-8. Available: <http://www.cptec.inpe.br/products/climanalise/capa1.html>.

CPTEC/INPE. *Resumo de eventos significativos em setembro de 2007*, 2007. Available: <http://www7.cptec.inpe.br/~rupload/figcartas/resumo_mensal/set07/cas_sig_setembro07.pdf>. Accessed: 07 mar. 2017.

DEKKER, A. G.; VOS, R. J.; PETERS, S. W. M. Comparison of remote sensing data, model results and in situ data for total suspended matter (TSM) in the southern Frisian lakes**.** *Sci. Total Environ.*, v. 268, n. 1-3, p. 197-214, 2001.

DHN – Diretoria de Hidrografia e Navegação. *Port of Santos Nautical Charts (Carta Náutica do Porto de Santos)*. Rio de Janeiro: Marinha do Brasil, Divisão de Hidrografia e Navegação, 2003.

DOERFFER, R.; FISCHER J.; STÖSSEL, M.; BROCKMANN, C.; GRASSL, H. Analysis of thematic mapper data for studying the suspended matter distribution in the coastal area of the German Bight (North Sea). *Remote Sens. Environ.*, v. 28, p. 61-73, 1989.

DURAND, N.; FIANDRINO, A.; FRAUNIÉ, P.; OUILLON, S.; FORGET, P.; NAUDIN, J. J. Suspended matter dispersion in the Ebro ROFI: an integrated approach. *Cont. Shelf Res.*, v. 22, n. 2, p. 267-284, 2002.

FERRARI, G. M.; DOWELL, M. D. CDOM Absorption Characteristics with Relation to Fluorescence and Salinity in Coastal Areas of the Southern Baltic Sea. *Estuar. Coast. Shelf Sci.*, v. 47, n. 1, p. 91-105, 1998.

FERRARI, A.; CIOTTI, A. M.; GIANNINI, M. F. C. Variability in the light absorption coefficients of phytoplankton, non-algal particles, and colored dissolved organic matter in a subtropical bay (Brazil). *Estuar. Coast. Shelf Sci.*, v. 139, p. 127-136, 2014.

FETTWEIS, M.; FRANCKEN, F.; PISON, V.; VAN DEN EYNDE, D. Suspended particulate matter dynamics and aggregate sizes in a high turbidity area. *Mar. Geol.*, v. 235, n. 1-4, p. 63-74, 2006.

FISCHER, J.; DOERFFER, R. An inverse technique for remote detection of suspended matter, phytoplankton and yellow substance from CZCS measurements. *Adv. Space Res.*, v. 7, n. 2, p. 21-26, 1987.

FORGET, P.; OUILLON, S. Surface suspended matter off the Rhone river mouth from visible satellite imagery. *Oceanol. Acta*, v. 21, n. 6, p. 739-749, 1998.

FRANCO, A. S. *Tides - fundamentals, analysis and prediction*. 2nd ed. São Paulo: FCTH, 1988. 249 p.

GASPARRO, M. R.; SOUSA, E. C. P. M.; GIORDANO, F.; ARGENTINO-SANTOS, R. C. Occupation history of the Santos estuary. In: RAMIRO NEVES, R.; BARETTA, J.; MATEUS, M. (Eds.). *Perspectives on Integrated Coastal Zone Management in South America*. Lisbon: IST Press, 2008. 603 p.

GEYER, W. R. Influence of Wind on Dynamics and Flushing of Shallow Estuaries. *Estuar. Coast. Shelf Sci.*, v. 44, n. 6, p. 713-722, 1997.

GODIN, G. (1972) *The analysis of tides*. Liverpool: Liverpool University Press, 246 p.

GREEN, E. P.; MUMBY, P. J.; EDWARDS, A. J.; CLARK, C. D.; EDWARDS A. J. (Ed). *Remote Sensing Handbook for Tropical Coastal Management.* Coastal Management Sourcebooks 3. Paris: UNESCO, 2000. 316 p.

HARARI, J.; CAMARGO, R.; FRANÇA, C. A. S.; MESQUITA, A. R.; PICARELLI, S. S. Numerical Modeling of the Hydrodynamics in the Coastal Area of Sao Paulo State Brazil. *J. Coast. Res.*, v. 3, n.si. 39, p. 1560-1563, 2006.

HARARI, J.; FRANÇA, C. A. S.; CAMARGO, R. Climatology and Hydrography of Santos Estuary. In: RAMIRO, N. R.; BARETTA, J.; MATEUS, M. (Eds.). *Perspectives on Integrated Coastal Zone Management in South America*. Lisbon: IST Press, 2008. 603 p.

INPE. CBERS – Satélite Sino-Brasileiro de Recursos Terrestres. 2011. Available: <http://www.cbers.inpe.br>. Accessed: 07 mar. 2017.

INTERNATIONAL OCEAN-COLOUR COORDINATING GROUP (IOCCG). Remote Sensing of Ocean Colour in Coastal, and Other Optically-Complex, Waters. In: SATHYENDRANATH, S. (Ed.). *Reports of the International Ocean-Colour Coordinating Group, n. 3*. Dartmouth: IOCCG, 2000.

KALNAY, E.; KNAMITSU, M.; KLISTER, R.; COLLINS, W.; DEAVEN, D.; GANDIN, I.; IREDELL, M.; SAHA, S.; WHITE, G.; WOOLLEN, J.; ZHU, Y.; CHELLIAH, M.; EBISUZAKI, W.; HIGGINS, W.; JANOWISK, J.; MO, K. C.; ROPELEWSKI, C.; WANG, J.; LEETMAA, A.; REYNOLDS, R.; JENNE, R.; JOSEPH, D. The ncep/ncar 40-year reanalysis project. *Bull. Am. Meteorol. Soc.*, v. 77, n. 3, p. 437-470, 1996.

MILLER, R. L.; MCKEE, B. A. Using MODIS Terra 250 m imagery to map concentrations of total suspended matter in coastal waters. *Remote Sens. Environ*., v. 93, n. 1-2, p. 259-266, 2004.

MILLER, R. L.; DEL CASTILLO, C. E.; CHILMAKURI, C.; MCCORQUODALE, J. A.; GEORGIOU, I.; MCKEE, B. A.; D'SA, E. J. Using multi-temporal MODIS 250 m data to calibrate and validate a sediment transport model for environmental monitoring of coastal waters. In: *Analysis of Multi-Temporal Remote Sensing Images. International Workshop on the Analysis of Multi-Temporal Remote Sensing Images, 2005*. p. 200-204. Available:<http://ieeexplore.ieee.org/stamp/stamp.jsp?arnumber=1469872&isnumber=31478>. Accessed: 07 mar. 2017.

MILLER, R. L.; LIU, C. C.; BUONASSISSI, C. J.; WU, A. M. A Multi-Sensor Approach to Examining the Distribution of Total Suspended Matter (TSM) in the Albemarle-Pamlico Estuarine System, NC, USA. *Remote Sens.*, v. 3, n. 5, 962-974, 2011.

MOSER, G. A. O.; GIANESELLA, S. M. F.; ALBA, J. J. B.; BÉRGAMO, A. L.; SALDANHA-CORRÊA, F. M. P.; MIRANDA, L. B.; HARARI, J. Instantaneous transport of salt, nutrients, suspended matter and clorophyll-a in the tropical estuarine system of Santos. *Braz. J. Oceanogr.*, v. 53, n. 3/4, p. 115-127, 2005.

MOSER, G. A. O.; CIOTTI, A. M.; GIANNINI, M. F. C.; TONINI, R. T.; HARARI, J. Changes in phytoplankton composition in response to tides, wind-induced mixing conditions and freshwater outflows in an urbanized estuarine complex. *Braz. J. Biol.*, v. 72, n. 1, p. 97-111, 2012.

NITTROUER, C. A.; WRIGHT, L. D. Transport of particles across continental shelves. *Rev. Geophys.*, v. 32, n. 1, p. 85-113, 1994.

ONDRUSEK, M.; STENGEL, E.; KINKADE, C. S.; VOGEL, R. L.; KEEGSTRA, P.; HUNTER, C.; KIM, C. The development of a new optical total suspended matter algorithm for the Chesapeake Bay. *Remote Sens. Environ.*, v. 119, p. 243-254, 2012.

OUBELKHEIR, K.; CLEMENTSON, L. A.; WEBSTER, I. T.; FORD, P. W.; DEKKER, A. G.; RADKE, L. C.; DANIEL, P. Using inherent optical properties to investigate biogeochemical dynamics in a tropical macrotidal coastal system. *J. Geophys. Res.*, v. 111, n. C7, p. 1-15, 2006.

PHINN, S. R.; DEKKER, A. G.; BRANDO, V. E.; ROELFSEMA, C. M. Mapping water quality and substrate cover in optically complex coastal and reef waters: an integrated approach. *Mar. Pollut. Bull.*, v. 51, n. 4-1, p. 459-469, 2005.

PULS, W.; DOERFFER, R.; SUNDERMANN, J. Numerical simulation and satellite observations of suspended matter in the North Sea. *IEEE J. Ocean Engineer.*, v. 19, n. 1, p. 3-9, 1994.

SANTOS, J. R.; MALDONADO, F. D.; GRAÇA, P. M. L. A. Integração de imagens LANDSAT/ETM+ e CBERS-2/CCD para detecção de mudanças em área da Amazônia sob domínio da floresta de transição. *Rev. Bras. Cartogr.*, v. 57, n. 1, p. 15-21, 2005.

SANTOS, A. R.; PELUZIO, T. M. O.; SAITO, N. S. *Spring 5.1.2: Passo a passo: Aplicações práticas*. Alegre: CAUFES, 2010. 153 p.

SCHMIEGELOW, J. M. M.; GIANESELLA, S. M. F.; SIMONETTI, C.; SALDANHA-CORREA, F. M. P.; FEOLI, E.; SANTOS, J. A. P.; SANTOS, M. P.; RIBEIRO, R. B.; SAMPAIO, A. F. P. Primary Producers In Santos Estuarine System. In: NEVES, R.; BARETTA, J.; MATEUS, M. (Eds.). *Perspectives on Integrated Coastal Zone Management in South America*. Lisbon: IST Press, 2008. 603 p.

SHI, W.; WANG, M. Satellite observations of flood-driven Mississippi River plume in the spring of 2008. *Geophys. Res. Lett.*, v. 36, n. 7, 2009.

SIEGEL, H.; GERTH, M.; MUTZKE, A. Dynamics of the Oder river plume in the Southern Baltic Sea: satellite data and numerical modeling. *Cont. Shelf Res.*, v. 19, n. 9, p. 1143-1159, 1999.

SIPELGAS, L.; RAUDSEPP, U.; KÕUTS, T. Operational monitoring of suspended matter distribution using MODIS images and numerical modelling. *Adv. Space Res.*, v. 38, n. 10, p. 2182-2188, 2006.

TANRÉ, D.; DEROO, C.; DUHAUT, P.; HERMAN, M.; MORCRETTE, J. J. Technical note Description of a computer code to simulate the satellite signal in the solar spectrum: the 5S code. *Int. J. Remote Sens.*, v. 11, n. 4, p. 659-668, 1990.